Far-infrared magnetoabsorption studies of zero-gap $Hg_{1-x}Mn_xSe$ crystals

A. M. Witowski
Institute of Experimental Physics, Warsaw University, Hoza 69, 00-681 Warsaw, Poland

J. K. Furdyna
Department of Physics, University of Notre Dame, Notre Dame, Indiana 46556

(Received 14 April 1993)

The results of magnetotransmission measurements performed on $Hg_{1-x}Mn_xSe$ crystals ($0.021 \leq x \leq 0.05$) at different temperatures are presented. The investigated materials have an inverted band structure (like HgSe). Most of the observed features are explained by transitions between conduction-band Landau levels, described by the Pidgeon-Brown model extended to include exchange interaction. The obtained values of the interaction gap E_0 and matrix element P complement results obtained from transport and interband magnetotransmission measurements, and show a nonlinear behavior of E_0 vs Mn composition x and a strong nonmonotonic dependence of P on x. The temperature dependence of Landau-level energies at low temperatures (between 2 and 8 K) is due to the changes of magnetization with temperature. In addition to spin and combined resonances, transitions allowed by warping and/or inversion asymmetry such as the second and third cyclotron harmonics are observed. The transitions, which could not be explained by transitions between Landau levels, are attributed to transitions from an impurity level (probably an ionized acceptor state) resonant with the conduction band. The zero-field energy of the level is estimated to be 3.8 meV above the top of the valence band.

I. INTRODUCTION

The ternary compound $Hg_{1-x}Mn_xSe$ belongs to the group of so-called diluted magnetic semiconductors (DMS's), investigated in the past few years.[1] These materials are characterized by the presence of a strong spin-spin exchange interaction between the localized magnetic moments of Mn^{2+} ions and the band electrons.[1] As a result of this interaction, extremely large and strongly temperature-dependent spin splitting of Landau levels is observed.[2-4]

In this paper the results of magnetotransmission measurements done for crystals with x greater than 0.02 and less than 0.06 are presented. $Hg_{1-x}Mn_xSe$ crystals with small manganese content have an inverted band structure (zero-gap materials). Selenium compounds (such as HgSe, CdSe, and mixed crystals) are always n type. The main technological goal is to obtain samples with a reasonably low free-carrier concentration. This means that the plasma edge cutoff occurs below the energy of far-infrared (FIR) laser light used. The technique of obtaining such samples, experimental details, and experimental results are described in Sec. II. In the next section the theory applied to the interpretation of the mentioned results is briefly reviewed. This theory explains the behavior of Landau levels for DMS and shows possible optical transitions between these levels.

The results obtained in this work allowed an analysis of band-structure parameters: the interaction energy gap E_0 and the momentum matrix element P as functions of manganese composition (Sec. IV). It should be pointed out that there exist only two papers[3,5] with data concerning the above-mentioned dependence for $Hg_{1-x}Mn_xSe$. Our data thus substantially extends the available information. In the same section, the temperature dependences of magnetic susceptibilities obtained from a fitting procedure to our data for different compositions are also presented.

The origin of some additional structures observed in magnetotransmission data and the mechanisms which could allow transitions leading to these structures are discussed in Sec. V. Most of them are explained by introducing an additional impurity level—probably an ionized acceptor level.

II. EXPERIMENTAL TECHNIQUE AND RESULTS

A. Samples and experimental setup

The $Hg_{1-x}Mn_xSe$ crystals used in these investigations were grown by the modified Bridgman method. The manganese compositions were obtained from the density of the specimens (see Table I). The samples were mechanically polished down to about 100 μm and etched in 10–15 % bromine-methanol solution to a thickness of about 50 μm. They were then annealed in dynamic vacuum at about 190 °C for 24 h. Prior to the FIR transmission measurements the samples were etched again to a final thickness of about 30 μm. Samples prepared in this way were mounted in special sample holders to avoid mechanical stresses during cooling and during measurements at low temperatures. The part of the sample surface which transmitted light was between 3 and 10 mm^2.

The measurements were carried out in a magnetic field up to 2.5 T using a conventional electromagnet. For one

TABLE I. The composition of used samples, obtained from density measurements.

Sample	A	$C5$	$C3$	$B7a$	$A3$
Composition	0.02	0.027	0.028	0.049	0.05

sample ($C3$) measurements were additionally performed in a superconducting coil at fields up to 8 T. The source of the FIR radiation was an optically pumped FIR laser operating at 96.5 μm (12.84 meV), 118.8 μm (10.43 meV), 163.0 μm (7.6 meV), and 170.0 μm (7.3 meV). Further details about the experimental procedure and experimental setup can be found elsewhere.[4,6] The measurements were carried out in the parallel Voigt ($\mathbf{B}\perp\mathbf{q}$ and $\mathbf{E}\|\mathbf{B}$, where $\mathbf{B}$ is the external magnetic field, $\mathbf{E}$ is the electric field of FIR radiation, and $\mathbf{q}$ is the light wave vector) and in the Faraday ($\mathbf{B}\|\mathbf{q}$) geometries, the latter employing in some experiments (mainly at 4.2 K) both circular polarizations. Part of the measurements were performed at temperatures between 2 and 8 K. The 8-K limit is due to the sharp decrease of the bolometer sensitivity.

B. The plasma effects

The main differences of transmission vs B for different samples are caused by changes of the plasma energy $\hbar\omega_P$. To illustrate this, in Fig. 1 the transmission data for the 118.8-μm laser line are compared for three samples with different $\hbar\omega_P$. When the plasma energy is smaller than the photon energy, the sample is transparent even at zero magnetic field [sample $C5$ with estimated $\hbar\omega_P \approx 9.6$ meV, see Fig. 1(c)]. In Fig. 1(b) the situation when plasma energy is only slightly greater than the photon energy is presented (sample $A3$ with $\hbar\omega_P \approx 10.5$ meV). In such a case, the sample is opaque at zero B (strong free-carrier absorption and medium value of reflectivity), but becomes transparent at a very low field for the cyclotron resonance inactive (CRI) circular polarization. Such behavior is well explained by the free-carrier dielectric function.[7] For higher plasma energy, a higher magnetic field is needed to open the transmission for CRI polarization [Fig. 1(a), sample A with $\hbar\omega_P \approx 11.5$ meV]. An analysis of the dynamic dielectric function[7] shows that conditions could exist in which a sample could be transparent for the cyclotron resonance active (CRA) polarization at lower magnetic field than for CRI polarization. Such a case was not observed in our experiments. Since for sufficiently large $\hbar\omega_P$ the real part of the dielectric function is negative over a broad range of magnetic fields in the vicinity of the cyclotron resonance,[7,4] the data for the CRA polarization (Fig. 2) do not show a cyclotron resonance (CR) line, but rather a broad cutoff band. The high-field end of the band is at the field, at which the cyclotron energy becomes equal to the photon energy.[7]

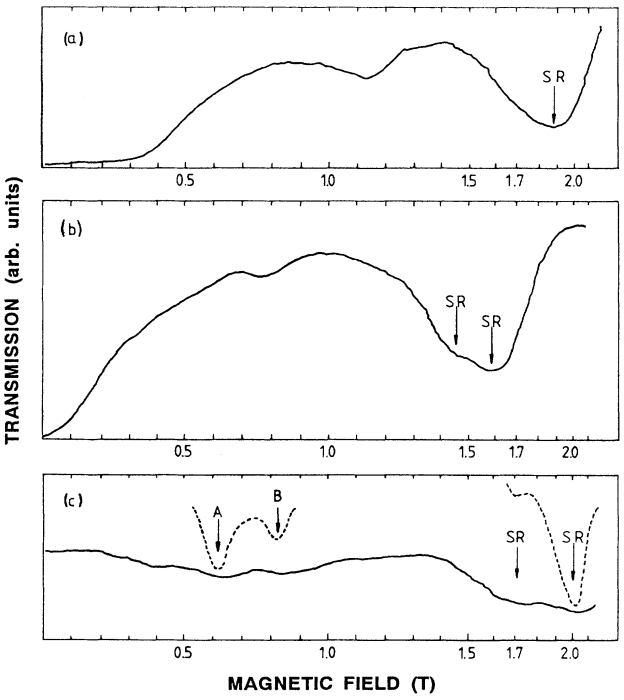

FIG. 1. The magnetotransmission curves taken using the 118.8-μm FIR laser line (photon energy $\hbar\omega = 10.43$ meV) at about 4.2 K in the Faraday configuration with linearly polarized light for (a) sample A with $\hbar\omega_P \gg \hbar\omega$, (b) sample $A3$ with $\hbar\omega_P \approx \hbar\omega$; (c) sample $C5$ with $\hbar\omega_P < \hbar\omega$. SR denotes the position of spin resonance and A and B positions of additional structures (details in text).

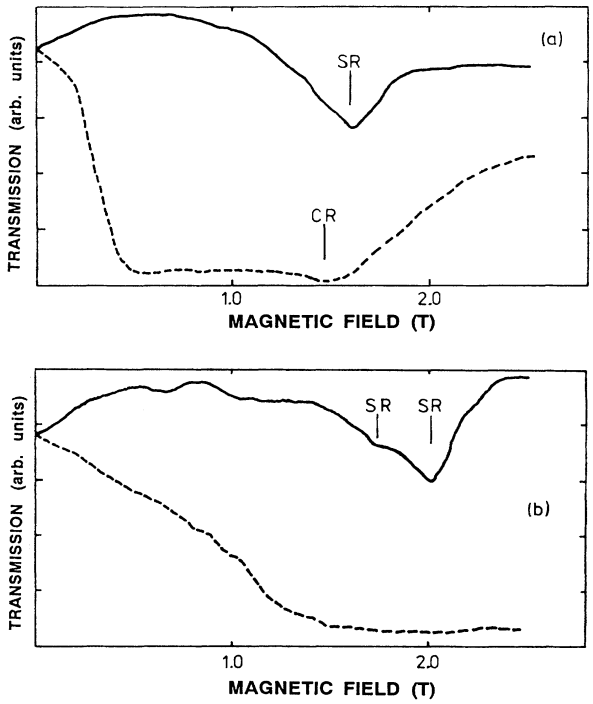

FIG. 2. The magnetotransmission curves taken using the 118.8-μm FIR laser line at about 4.2 K in the Faraday configuration for both circular polarizations: CRI (solid line) and CRA (dashed line). (a) data for sample $B7a$ ($x = 0.049$), (b) data for sample $C3$ ($x = 0.028$). SR and CR denote the positions of spin and cyclotron resonances, respectively.

C. Absorption lines

In the regions of magnetic field and photon energy where samples were transparent, the absorption due to the electric dipole excited spin resonance (SR) was observed in the CRI polarization[4,6,8] (lines marked SR in Figs. 1 and 2). For a low concentration of magnetic ions (less than about 1%) in DMS the spin splitting is smaller than the cyclotron splitting, but for 2–4 % of manganese the opposite is true ($\hbar\omega_{CR} < \hbar\omega_{SR}$). This is illustrated in Fig. 2 (compare data for CRI and CRA polarizations). When the content of magnetic ions is greater than 4%, we observe the same order of splitting as for low compositions (data for sample $B7a$ in Fig. 2, $\hbar\omega_{CR} > \hbar\omega_{SR}$). This change is near the crossover point between the inverted and open gap band structures, where the effective mass becomes very small. After passing this point the effective g factor is affected by the negative exchange integral (Sec. III) and this can lead even to a change of sign of the g factor for higher Mn compositions ($x > 0.12$).[9] Since the spin splitting of Landau levels depends strongly on temperature, the above-mentioned features exist at low temperature only. At a sufficiently high temperature $\hbar\omega_{CR} > \hbar\omega_{SR}$ for all compositions.

As an example of the temperature dependence of the Landau-level splittings, the positions of spin and combined resonances vs temperature for one of the samples in question are presented in Fig. 3.

As mentioned earlier, the additional measurements up to 8 T were done in the Voigt configuration for sample $C3$. The results are shown in Fig. 4. At about 1 T a sharp line due to the combined resonance is observed. The strong electric dipole excited SR is also seen. Its double structure (line B) is confirmed by measurements using a conventional electromagnet [see Fig. 2(b)]. This line changes its position with temperature and is stronger at higher T. The origin of two weak lines about 4–5 T (I_0 and I_1), vanishing at 7 K, will be discussed in Sec. V.

III. THEORY

The description of the electronic states of diluted magnetic semiconductors in the presence of a magnetic field B is obtained by introducing the spin-spin exchange interaction as an additive term to the well-known Hamiltonian of nonmagnetic narrow-gap semiconductors. This Hamiltonian is described (for example) by the Pidgeon-Brown (PB) model.[10] In the model the problem of an electron in a magnetic field is treated in terms of the effective-mass approximation, taking into account the contributions of the neighboring Γ_6, Γ_7, and Γ_8 bands exactly, and treating the remaining "higher" bands in an approximate way. This model was reviewed in detail by Aggarwal.[11] For $k_z = 0$, the Hamiltonian separates into two 4×4 matrices: D_a and D_b corresponding to the "quasi-spin-up" and "quasi-spin-down" states, respectively. Since our interest is the conduction band in zero-gap $Hg_{1-x}Mn_xSe$ we can make the following simplifications: (1) assuming Γ_8 bands to be spherically symmetric, we can take $\gamma_2 = \gamma_3 = \gamma$, and (2) since F affects only the Γ_6 band,[10] in our analysis of the Γ_8 conduction band we set $F = 0$.

The properties of DMS are also strongly affected by the exchange interaction between the band electrons and the $3d$ electrons of the Mn^{2+} ions. The effect of this interaction on electronic states could be taken into account by adding an exchange term (in the Heisenberg form)[12,13] to the nonmagnetic PB Hamiltonian. In terms of the virtual crystal- and molecular-field approximations the exchange Hamiltonian is given by

$$H_{ex} = x\sigma_z \langle S_z \rangle \sum_{\mathbf{R}} J(\mathbf{r}-\mathbf{R}) , \tag{1}$$

where σ_z is the spin operator of band electrons, $\langle S_z \rangle$ is the thermal average of manganese spin in the paramagnetic system with a magnetic field applied in the z direction, $\mathbf{R}$ denotes the coordinate of every site of the Mn-Hg fcc sublattice, J is a function describing the electron-ion exchange coupling, and $\mathbf{r}$ is the coordinate of the band electron.

The advantage of the above approximations is that Eq. (1) has the periodicity of the lattice and is thus tractable within the framework of Bloch solutions, enabling the solutions of the total Hamiltonian $\mathbf{H}$ [which includes Eq. (1)] to be expressed in terms of the same basis functions as those of the PB model. Using these basis functions one then obtains the additional 4×4 "a" and "b" matrices D_a^{ex} and D_b^{ex} representing the exchange contributions. Among the numerical coefficients in these matrices are the following values $N_s\alpha\langle S_z \rangle$ and $N_s\beta\langle N_z \rangle$, where $N_s = xN_0$ (N_0 is the number of unit cells per unit

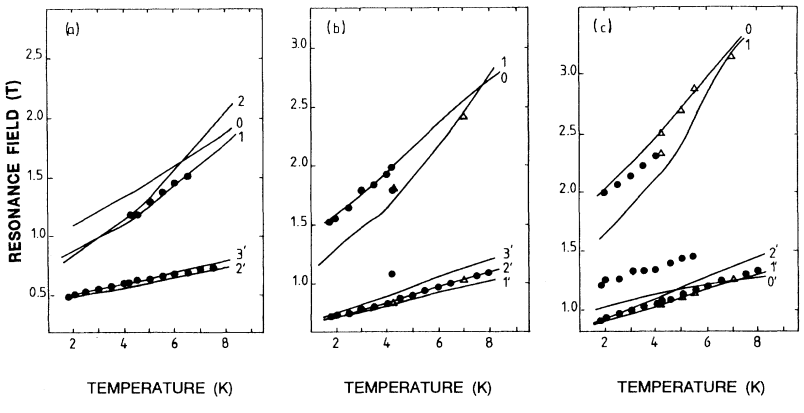

FIG. 3. The positions of spin and combined resonances vs temperature for sample $C3$ and various FIR laser lines. (a) 163.0-μm line (7.6 meV), (b) 118.8-μm line (10.43 meV), (c) 96.5-μm line (12.84 meV). Points and triangles represent experimental data obtained in low magnetic-field experiments and high magnetic-field measurements, respectively. The solid lines represent the theoretical dependence calculated for magnetic susceptibility depicted in Fig. 6. n' denotes the combined resonances due to the $a(n') \rightarrow b(n'+1)$ transitions, and n spin-flip transitions $a(n) \rightarrow b(n)$.

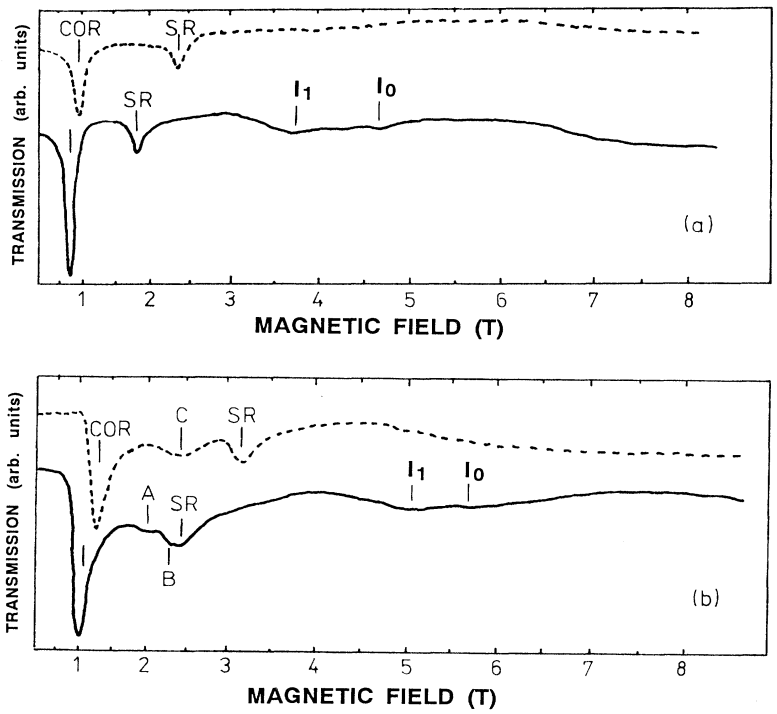

FIG. 4. The magnetotransmission curves obtained in the parallel Voigt geometry at about 4.2 K (solid line) and at about 7 K (dashed line) for photon energies. (a) 10.35 meV, (b) 12.84 meV. SR and COR denote spin-flip and combined resonances, respectively. *A*, *B*, *C*, I_0, and I_1 mark additional resonances (unexplained by the simple PB model).

volume), and $\alpha=\langle S|J|S\rangle$ and $\beta=\langle X|J|X\rangle$, the exchange integrals corresponding to the Γ_6 (*S*-type) and Γ_8 (*P*-type) bands, respectively.

The average value of spin $\langle S_z\rangle$ is related to the magnetization M of the material in question by

$$M=N_s g\mu_B\langle S_z\rangle \ . \tag{2}$$

Here, g is the manganese g factor (taken equal to 2 following Ref. 14) and μ_B is the Bohr magneton. $\langle S_z\rangle$ can be obtained directly from magnetization measurements or (for low B) from magnetic susceptibility data. One can also treat $\langle S_z\rangle$ as a fitting function. The other possibility is to take a theoretical model of magnetization, e.g., that proposed by Gaj, Planel, and Fishman.[15] In the framework of this model (for paramagnetic materials) the average value of the spin $\langle S_z\rangle$ can be written as

$$\langle S_z\rangle=-S_0 B_S(t) \ , \tag{3}$$

where S_0 is the saturation spin value of manganese and $B_S(t)$ is the Brillouin function with argument $t=g\mu_B SB/[k_B(T+T_0)]$, where T is temperature, T_0 is an adjustable parameter, and $S=\frac{5}{2}$ for Mn^{2+}.

The full Hamiltonian, containing the Pidgeon-Brown treatment of the bands and the exchange contribution, can now be written as two sets of 4×4 matrices

$$\begin{aligned} D_a^f&=D_a+D_a^{\rm ex} \ , \\ D_b^f&=D_b+D_b^{\rm ex} \ . \end{aligned} \tag{5}$$

By diagonalizing these matrices one finds the energies of the Landau levels for $k_z=0$ at a given magnetic field. The described theoretical model has the following parameters: $E_0=E(\Gamma_6)-E(\Gamma_8)$ is the interaction energy gap at the Γ point, $P=i\hbar\langle S|p_z|Z\rangle/m_0$ is the momentum matrix element, $\Delta=E(\Gamma_8)-E(\Gamma_7)$ is the spin-orbit splitting at the Γ point, γ_1, γ, and κ are the "higher band" parameters, α and β are the exchange integrals defined earlier, and parameters describing $\langle S_z\rangle$ and/or magnetization.

Within the framework of this model there are three allowed transitions between the Landau levels, which can be observed in the FIR region: (a) cyclotron resonance (CR) elicited by the CRA circular polarization (Faraday geometry); (b) electric dipole excited spin resonance (SR) elicited by the CRI circular polarization when the effective g factor of the conduction electrons is negative (as in the case of zero-gap semiconductors) (Faraday geometry); and (c) combined resonance (COR) observed in the parallel Voigt ($\mathbf{E}\|\mathbf{B}$) geometry.

The CR is the only electric dipole transition allowed in a noninteracting isotropic single-electron band. The two other transitions mentioned above (SR and COR) are allowed in the presence of spin-orbit coupling when the selection rules which normally forbid these transitions become relaxed as a result of wave-function mixing through the kp interaction and/or inversion asymmetry.[6,16,17]

One of the more general theories which try to explain the mechanisms allowing others transitions such as cyclotron resonance harmonics was described by Weiler, Aggarwal, and Lax.[17] In order to find all allowed transitions for InSb among the conduction-band states, the authors of Ref. 17 obtained from the tables of Koster *et al.*[18] all allowed terms up to second order in k and to the first order in magnetic field B in the 8×8 matrix Hamiltonian for the Γ_6, two Γ_8 and the Γ_7 bands. The additional transitions found in Ref. 17 are induced by warping and by

inversion asymmetry. It should be pointed out that the corrections taken into account in Ref. 17 in the first approximation do not change the energy of Landau levels but only mix the wave functions from different states.

We fitted the theoretical values of the transition energies at $k_z=0$ for SR and COR at a given magnetic field to those found in the experiment. The fitting procedure was described in detail in Ref. 4. We used the following parameters from the literature: $\Delta=387$ meV, $\gamma_1=0.1$, $\gamma=0.2$, and $\kappa=-0.7$ obtained by Dobrowolska, Dobrowolski, and Mycielski[19] and Pastor, Jaczynski, and Furdyna[6] for HgSe, $\alpha N_0=340$ meV and $\beta N_0=-900$ meV as proposed for $Hg_{1-x}Mn_xSe$ by Byszewski, Cleplak, and Mongird-Gorska.[20]

IV. BAND-STRUCTURE PARAMETERS AND MAGNETIC SUSCEPTIBILITY

The electroreflectivity measurements done for $Hg_{1-x}Mn_xTe$ (Ref. 8) and interband magnetoabsorption data for $Hg_{1-x}Cd_xSe$ (Ref. 21) show that spin-orbit coupling and higher band parameters are practically composition independent, especially for low composition (few %). Thus, in the fitting procedure we used the same values of these parameters as for HgSe.

We chose three parameters, namely E_0, P, and T_0, as fitting parameters to the data at 4.2 K for various compositions [see Figs. 9 and 10(a) as examples]. Then we fitted only T_0 for given E_0 and P to the data at other temperatures (see, e.g., Fig. 3). We assume that E_0 and P are constant in the experimental temperature range. This allowed us to obtain the dependence of parameters E_0 and P on composition and the dependence of magnetic susceptibility (directly related to T_0) on temperature. The plots of the interaction energy gap E_0 and the momentum matrix element P vs manganese composition are shown in Fig. 5. For comparison, the data of Dobrowolska *et al.*[3] and Takeyama and Galazka[5] are enclosed in the same plot. One can see that our results essentially complete previous data, and allow us to establish the "crossover point" ($E_0=0$) at 4.2 K, at $x\approx0.055$ (transition from the inverted to the InSb-type band structure). The data obtained in this work confirm earlier suggestions that especially for low Mn compositions, the interaction energy gap is a nonlinear function of composition as in $Hg_{1-x}Mn_xTe$,[9] contrary to the behavior observed for $Hg_{1-x}Cd_xSe$ (Ref. 21) and $Hg_{1-x}Cd_xTe$ (Ref. 22) (linear dependence). The dependence of P on composition is nonmonotonic [Fig. 5(b)]. In the beginning the value of P decreases with increasing Mn concentration to reach a minimum value at about $x\approx0.04$ and then slowly increases or stays constant. This behavior is different even from that observed for $Hg_{1-x}Mn_xTe$,[9] where P first slowly increases and then decreases. It should be mentioned that for mixed crystals such as $Hg_{1-x}Cd_xSe$ (Ref. 21) and $Hg_{1-x}Cd_xTe$ (Ref. 22) P is a linear function of cadmium composition. These facts can suggest that the theory used to describe the energy of Landau levels in a magnetic field for zero- and narrow-gap diluted magnetic semiconductors is too simple. It should probably include

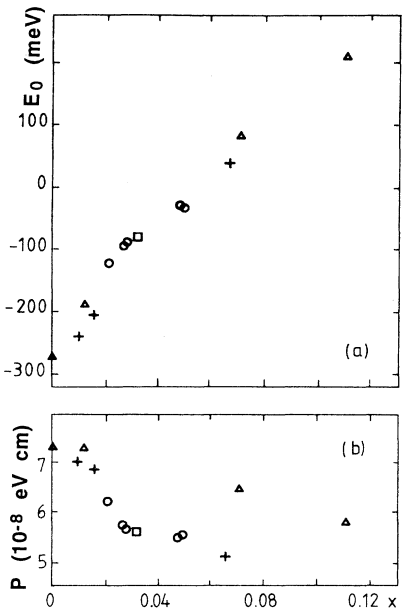

FIG. 5. (a) The dependence of the interaction energy gap E_0 on manganese composition. (b) The dependence of the momentum matrix element P on Mn content. Circles represent the data obtained in this work, the square is from our previous paper (Ref. 4), triangles are after Ref. 3, and crosses are after Ref. 5.

the interaction (hybridization) between the Γ_6, Γ_7, and Γ_8 bands with the manganese d level (or band). A more detail discussion on this subject has been presented by us in Ref. 23.

One can calculate from Eq. (2) the magnetic susceptibility as a function of temperature from the obtained dependence of T_0 on temperature. These data for various Mn compositions are presented in Fig. 6. They are in good agreement with the data obtained from direct susceptibility measurements[24] and data calculated from magnetization measurements.[25] This demonstrates that in the discussed temperature region the changes of SR and COR magnetic-field positions with temperature are due to the magnetization dependence on T. Such a good agreement can also be an argument for good fitting quality.

V. ADDITIONAL ABSORPTION STRUCTURES

A. Warping and inversion asymmetry

In Sec. IV we discussed what information can be obtained about the material in question from the resonances allowed in the simple PB model (SR and COR). Some extensions of the model were presented in Sec. III. These extensions explain additional resonances observed in magnetotransmission for InSb (Ref. 17) (e.g., double cyclotron resonance, $2\hbar\omega_{CR}$; triple CR, $3\hbar\omega_{CR}$; and spin-flip "assisted" double CR, $2\hbar\omega_{CR}+\hbar\omega_{SR}$. In our data for $Hg_{1-x}Mn_xSe$ some additional structures have also been

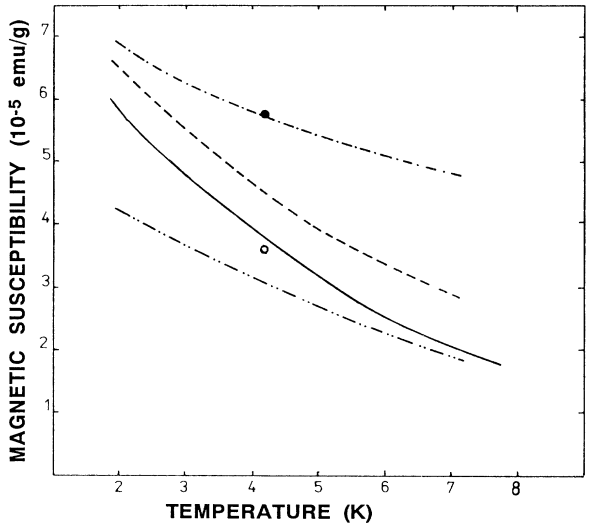

FIG. 6. The magnetic susceptibility as a function of temperature obtained from the fitting procedure to magnetotransmission data (details in text) for the following compositions: $x=0.021$ (sample A), $-\cdots-\cdots-$); $x=0.027$ ($C5$), ○; $x=0.028$ ($C3$), ——; $x=0.032$ (from Ref. 4) — — —; $x=0.049$ ($B7a$) —·—·—·; and $x=0.05$ ($A3$) ●.

observed. Some of them are due to the electric dipole excited SR allowed in the Voigt $\mathbf{E}\|\mathbf{B}$ configuration (Fig. 4). We will not discuss them here because there are many papers on this subject (e.g., Refs. 16 and 17) even for HgSe.[6,26] In Ref. 26 the authors show from the angular variation of SR intensity that the dominant mechanism allowing these transitions is the inversion asymmetry.

One of the other additional structures is the absorption line observed for sample A [Fig. 1(a)] at a magnetic field lower than the SR field. The dependence of the magnetic-field position of the line on T is shown in Fig. 7. The presented temperature behavior differs significantly from that of SR and COR (compare Figs. 3 and 7). Such a weak dependence on T suggests that the cyclotron resonance could be involved in this transition. The energy of double cyclotron transitions ($2h\omega_{CR}$) possible for a particular Fermi level were calculated for the previously obtained parameters E_0, P, and T_0. The magnetic field at which those transitions occur for photon energies of 10.43 and 12.84 meV vs temperature are plotted in Fig. 7. As one can see, the agreement with the experimental data is very good, but one cannot establish which transition plays the dominant role in observed absorption line. It is probably a combination of all the transitions possible for a given Fermi energy, with their intensities varying with temperature.

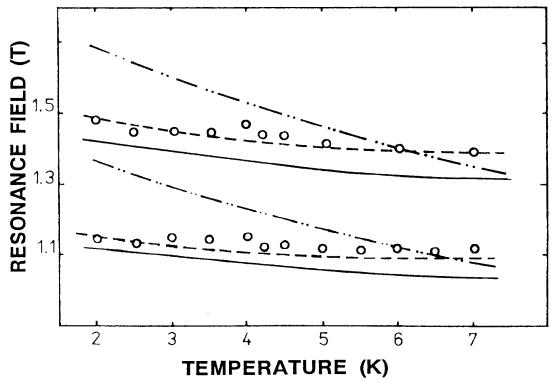

FIG. 7. The dependence of the magnetic-field positions of additional absorption lines for sample A [see Fig. 1(a)] on temperature for photon energy. 12.84 meV, upper part; 10.43 meV, lower part. The curves show the theoretically obtained temperature dependence of double cyclotron resonances. $b(0)\rightarrow b(2)$ and $a(1)$, $\rightarrow a(3)$, solid line; $b(1)\rightarrow b(3)$, dashed line; and $a(0)\rightarrow a(2)$, dot-dashed line.

An especially rich spectrum of additional structures is observed for samples $C5$ and $C3$ [Figs. 1(c) and 4], but the lack of data at different temperatures does not allow a full verification of the explanation of the origin of these lines presented below.

The magnetotransmission curve obtained in the Faraday geometry for sample $C5$ [Fig. 1(c)] shows two absorption lines marked as A and B. They appear at about 0.8 T for the laser line 118.8 μm and at about 0.9 T for line 96.5 μm. One can also observe some additional lines in

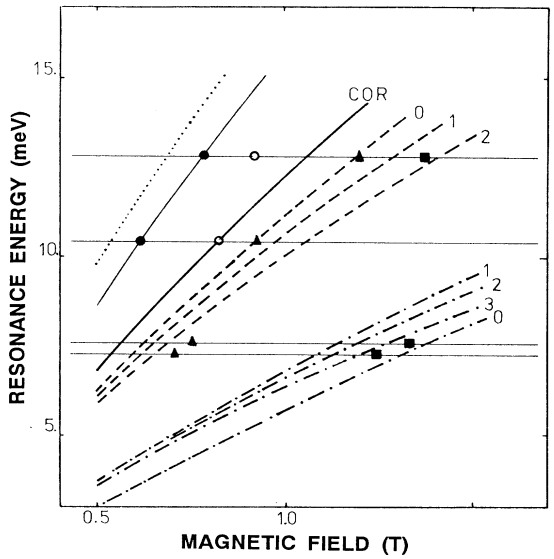

FIG. 8. The energies of resonances unexplained by the Pidgeon-Brown model vs magnetic field at 4.2 K for sample $C5$. The dotted line represents the $2\omega_{CR}+\omega_{SR}$ transition between levels $a_c(0)$ and $b_c(2)$ and/or levels $a_c(1)$ and $b_c(3)$. The light solid line represents a $3\omega_{CR}$ transition from level $a_c(0)$ to $a_c(3)$ (all other triple cyclotron resonances have lower energies). The heavy solid line denotes the highest energy for COR ($\omega_{CR}+\omega_{SR}$) resonances, i.e., the transition from level $a_c(1)$ to $b_c(2)$. The broken lines denote double cyclotron transitions between levels $b_c(n)$ and $b_c(n+2)$ (compare with Fig. 7). The dashed dotted lines describe the spin-flip transition inside the nth level. The circles represent experimental points obtained in the Faraday geometry. ●, line A; ○ line B [see Fig. 1(c)]; ■; satellite to SR lines; and ▲ denote experimental data obtained in the Voigt parallel geometry.

the Voigt geometry. The energies of all these unexplained transitions vs B are shown in Fig. 8. Lines presented in the same figure describe the theoretical dependence of the energies of $2\hbar\omega_{CR}$ and $3\hbar\omega_{CR}$ on magnetic field. Almost all absorption lines, except line B, can be explained by these cyclotron resonance harmonics. One can try to describe it as due to the transition from the $a_c(-1)$ level to the $b_c(1)$ level $(2\hbar\omega_{CR}+\hbar\omega_{SR})$ for the photon energy equal to 12.84 meV and as COR allowed in the Faraday geometry for the photon energy of 10.43 meV.

We could not explain the satellites to SR lines observed for the photon energies 7.3 and 7.6 meV. Such lines were also observed previously for the sample with $x=0.032$.[4] Their unusual temperature dependence was presented earlier.[4] It should be stressed that these structures have no explanation even assuming the existence of an additional impurity level.

Another unexplained absorption line is that observed for the photon energy 12.84 meV at about 1.35 T in the magnetotransmission for sample $C3$ investigated in the Voigt configuration (Fig. 3). The position of this transition could suggest that it is a double cyclotron resonance, but the temperature behavior of the magnetic field at which the line is observed is similar to that of COR and does not confirm this suggestion.

B. Impurity level

Let us take into account an additional impurity level. In zero-gap semiconductors only acceptor impurities can give localized states (ionization energy E_A is the energy between the level and the Γ_8 valence band).[27,28] These states are resonant with the conduction Γ_8 band.[29–34] In HgSe and ternary compounds based on it all such states should be ionized due to the relatively high value of the Fermi energy ($E_F > E_A$). Up to now, there are no experimental data about the energy of such levels in mercury selenide, however there are some experimental evidences

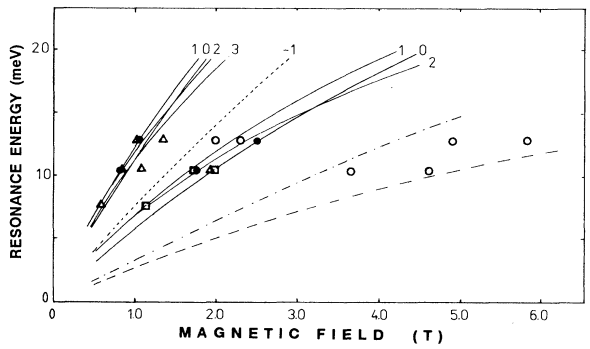

FIG. 9. The energies of various transitions vs magnetic field for sample $C3$ at about 4.2 K. Horizontal lines represent energies of FIR laser lines. Circles describe the positions of resonances observed in the Voigt parallel geometry (Fig. 4) (open unexplained by PB model). Squares represent positions of absorption lines observed in the Faraday configuration. Triangles denote the positions of resonances observed in the Voigt parallel configuration observed at low magnetic-field experiments. Lines describe the theoretical positions of resonances. ——, spin flip inside nth level (low energies) and combined resonance $a_c(n)\rightarrow b_c(n+1)$ (high energies); ----, combined resonance $a_c(-1)\rightarrow b_c(0)$ transition; —·—·—, the lowest energy of interband transitions, transition $b_v(1)\rightarrow a_c(0)$; — — —, the lowest spin-flip resonance energy (inside -1 level). Compare these data with Fig. 10(a).

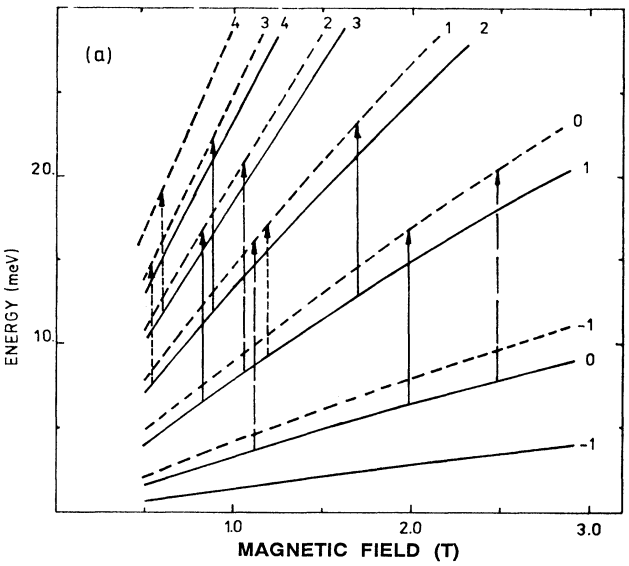

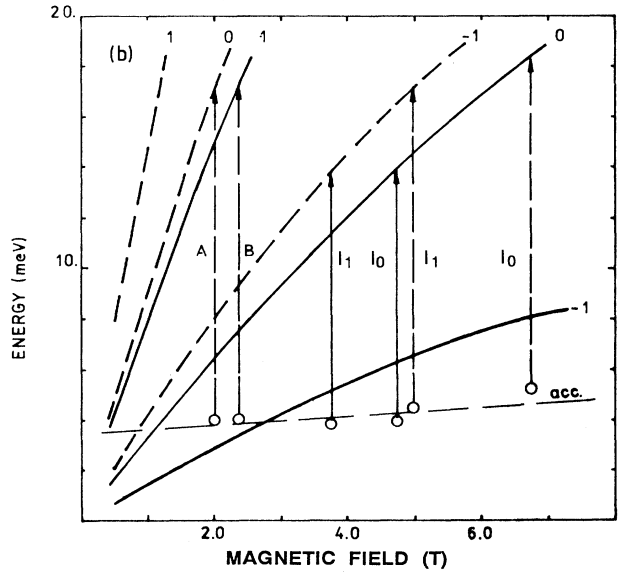

FIG. 10. The energies of Landau levels at $k_2=0$ as functions of the magnetic field calculated for parameters for sample $C3$ at 4.2 K. The different transitions with different energies are shown by the arrows. (a) Transitions between Landau levels for photon energies. 12.84 meV (96.5 μm) (broken arrows); 10.43 meV (118.8 μm) (solid arrows); and 7.6 meV (163.0 μm) (dashed arrows). (b) Transitions from the hypothetical acceptor level to the Landau levels. They are marked in the same manner as absorption lines in Fig. 4. Notation of transition energies is as in Fig. 10(a).

for the existence of an impurity level in these materials.[35–38] One can expect that for mixed crystals based on HgSe, such as $Hg_{1-x}Mn_xSe$, it is possible to find transitions from an ionized acceptor level(s) to conduction-band states as for HgTe (Ref. 32) and $Hg_{1-x}Mn_xTe$.[39] Thus, the intraband magnetotransmission measurements are the most promising experiments for finding the above-mentioned transitions.

In the magnetotransmission results for sample $C3$ (Fig. 4), one can see two weak lines (I_1 and I_0) occurring at about 4 T for photon energy 10.43 meV and at about 5.5 T for 12.84 meV. These structures vanish at 7 K. Their energies are marked as open circles in Fig. 9. One can try to explain the transitions giving lines I_1 and I_0 as spin-flip transitions inside the (-1) Landau level and interband transitions from the $b_v(1)$ valence-band Landau level to the $a_c(0)$ conduction-band level (Fig. 9), respectively. To obtain a better agreement between theoretical and experimental energies of the above-mentioned transitions one has to change the band-structure parameters and/or magnetic parameters (β, T_0) so strongly that the other observed resonances (SR and COR) will become unexplained. If one assumes an additional impurity level [dashed line in Fig. 10(b)] the I_1 and I_0 lines will be well explained as being due to the transitions from this level to the $a_c(0)$ and $b_c(-1)$ levels, respectively. The A and B lines observed at 4.2 K for photon energy 12.84 meV, which were previously unexplained, will in such a case be due to transitions from the impurity level to the $b_c(0)$ and $a_c(1)$ Landau levels [see Fig. 10(b)], respectively. Since the spin splitting at higher temperatures is smaller and the Landau levels (at a given magnetic field) have smaller energy,[3] one can expect that all the above transitions should be weaker. This is caused by the larger population of the final levels at higher temperatures. Additionally, one can take into consideration the temperature broadening of levels. These two mechanisms could make the observation of the discussed transitions impossible. The positions of the transitions to $b_c(0)$ and $a_c(1)$ would be shifted to the higher magnetic fields and became broader with increasing temperature. This leads to the observation of only one broad line instead of two lines. These features can be seen comparing transmission curves taken at 4.2 and 7 K (Fig. 4).

One can notice in Fig. 10(b) that at magnetic fields above 2.6 T the impurity level moves below the valence-band levels $a_c(-1)$ and $b_c(-1)$. Such behavior is unusual for a neutral (unionized) acceptor level. For an ionized (as in our case) acceptor it is difficult to predict how its energy levels should behave in an external magnetic field B. On the other hand, it could also mean that the acceptor level is built from lower valence-band Landau levels (higher numbers) which lower their energies with increasing B. If one assumes a linear dependence of E_A vs B [as in $Hg_{1-x}Mn_xTe$ (Ref. 39)], then the zero-field energy of the impurity level is about 3.8 meV. It is substantially higher than that in $Hg_{1-x}Mn_xTe$ (Ref. 39) (2.2 meV). This should be pointed out, that the existence of ionized acceptor states can explain the existence of empty states on the level $b_c(-1)$ at 4.2 K.

VI. CONCLUSIONS

The results of magnetotransmission measurements performed on $Hg_{1-x}Mn_xSe$ crystals at different temperatures were presented. The content of manganese in the samples was between 0.021 and 0.05, which means that these materials have an inverted band structure (as HgSe).

The obtained data endorse once more the view that the temperature dependence of Landau levels energies at low temperatures (between 2 and 8 K) is due to the changes of magnetization with temperature. From the fitting of resonance positions obtained from a Pidgeon-Brown model (extended to include exchange interaction) to our results we obtained the values of the interaction gap E_0 and the momentum matrix element P for different manganese compositions. These data complement the results from transport and interband magnetotransmission measurements and show the nonlinearity of changes of E_0 vs Mn composition x and strong nonmonotonic behavior of P vs x. This is probably due to the hybridization of the Mn d level with the valence-band p states.

In addition to spin and combined resonances, transitions allowed by warping and/or inversion asymmetry, such as second and third cyclotron harmonics, were observed.

Transitions which could not be explained by the presented modified Pidgeon-Brown model were also observed. Most of them were explained by introducing an impurity level resonant with the conduction band. This is probably an ionized acceptor state. On the basis of the observed transitions one can estimate the dependence of the energy of this level on magnetic-field and zero-field energy of the level. This energy is estimated to be 3.8 meV above the bottom (top) of the conduction (valence) band. In some ranges of magnetic fields this level appears to be resonant with one of the valence-band Landau levels (which exhibits a magnetic-field behavior similar to the conduction-band levels). The assumption of the existence of such an impurity level also explains the temperature behavior of additional absorption lines. This is the first clear experimental evidence of an impurity level in zero-gap mixed crystals based on HgSe; however, such a level with an energy of about 2.2 meV has been observed in HgTe and $Hg_{1-x}Mn_xTe$. Observations of so many features were possible due to the good quality of the crystals used, which led to the required low free-carrier concentration. The presented analysis was not fully successful because of the unknown origin of certain absorption lines.

ACKNOWLEDGMENTS

The authors wish to thank Dr. M. Jaczynski for the crystal growth, and Professor M. Grynberg and Dr. M. Dobrowolska for valuable discussions. One of us (A.M.W.) wishes to thank Purdue University for the hospitality extended to him during the course of the FIR experiments. This work was supported in part by the National Science Foundation Grant Nos. MDR 8600014 and DMR 8712767.

[1]*Semiconductors and Semimetals,* edited by J. K. Furdyna and J. Kossut (Academic, New York, 1988), Vol. 25; J. K. Furdyna, J. Appl. Phys. **64**, R29 (1988).
[2]K. Pastor, M. Grynberg, and R. R. Galazka, Solid State Commun. **29**, 739 (1979); M. Jaczynski and W. D. Dobrowolski, Phys. Status Solidi B **102**, 195 (1980).
[3]M. Dobrowolska, W. Dobrowolski, R. R. Galazka, and A. Mycielski, Phys. Status Solidi B **105**, 477 (1981).
[4]A. Witowski, K. Pastor, and J. K. Furdyna, Phys. Rev. B **26**, 931 (1982).
[5]S. Takeyama and R. R. Galazka, Phys. Status Solidi B **96**, 412 (1979).
[6]K. Pastor, M. Jaczynski, and J. K. Furdyna, Phys. Rev. B **24**, 7312 (1981).
[7]E. D. Palik and J. K. Furdyna, Rep. Prog. Phys. **33**, 1193 (1970).
[8]P. M. Amirtharaj, F. H. Pollak, and J. K. Furdyna, Solid State Commun. **39**, 35 (1981).
[9]G. Bastard, C. Rigaux, Y. Guldner, A. Mycielski, J. K. Furdyna, J. Appl. Phys. **53**, 7637 (1982).
[10]C. R. Pidgeon and R. N. Brown, Phys. Rev. **146**, 575 (1966); W. Leung and L. Liu, Phys. Rev. B **8**, 3811 (1973).
[11]R. L. Aggarwal, in *Semiconductors and Semimetals,* edited by R. K. Willardson and A. C. Beer (Academic, New York, 1972), Vol. 9, p. 151.
[12]J. Kossut, Phys. Status Solidi B **78**, 537 (1976).
[13]G. Bastard, C. Rigaux, and A. Mycielski, Phys. Status Solidi B **79**, 585 (1977); G. Bastard, C. Rigaux, Y. Guldner, J. Mycielski, and A. Mycielski, J. Phys. (Paris) **39**, 87 (1978).
[14]R. T. Holm and J. K. Furdyna, Solid State Commun. **15**, 1459 (1974).
[15]J. A. Gaj, R. Planel, and G. Fishman, Solid State Commun. **29**, 435 (1979).
[16]B. D. McCombe, Phys. Rev. **181**, 1206 (1969).
[17]M. H. Weiler, R. L. Aggarwal, and B. Lax, Phys. Rev. B **17**, 3269 (1978).
[18]C. F. Koster, J. O. Dimmock, R. G. Wheeler, and H. Statz, *Properties of the Thirty Two Point Groups* (MIT, Cambridge, 1966).
[19]M. Dobrowolska, W. Dobrowolski, and A. Mycielski, Solid State Commun. **34**, 441 (1980).
[20]P. Byszewski, M. Z. Cieplak, and A. Mongird-Gorska, J. Phys. C **12**, 5383 (1980).
[21]A. Mycielski, J. Kossut, M. Dobrowolska, and W. Dobrowolski, J. Phys. C **15**, 3293 (1982).
[22]J. D. Wiley and R. N. Dexter, Phys. Rev. **181**, 1181 (1961).
[23]A. M. Witowski and J. K. Furdyna, in *Proceedings of the 19th International Conference on the Physics of Semiconductors,* edited by W. Zawadzki (Institute of Physics, Polish Academy of Sciences, Warsaw, 1988), p. 1579.
[24]G. D. Khattak, C. D. Amarasekara, S. Nagata, R. R. Galazka, and P. H. Keesom, Phys. Rev. B **23**, 3553 (1981).
[25]W. Dobrowolski, M. von Ortenberg, A. M. Sandauer, R. R. Galazka, A. Mycielski, and R. Pauthenet, in *Proceedings of the 4th International Conference on the Physics of the Narrow Gap Semiconductors,* edited by E. Gornik, H. Heinrich, and L. Palmetshofer, Lecture Notes in Physics Vol. 152 (Springer-Verlag, Berlin, 1982), p. 302.
[26]M. H. Weiler, M. Dobrowolska, A. M. Witowski, and J. K. Furdyna, Bull. Am. Phys. Soc. **28**, 419 (1983).
[27]I. M. Tsidilkowski, in *Proceedings of the Summer School on Narrow Gap Semiconductors, Physics and Applications,* edited by W. Zawadzki, Lecture Notes in Physics Vol. 133 (Springer-Verlag, Berlin, 1980), p. 324.
[28]In the case of DMS see, e.g., J. Mycielski, in *Applications of High Magnetic Fields in Semiconductor Physics,* edited by G. Landwehr (Springer-Verlag, Berlin, 1983), p. 431; A. M. Witowski, Acta Phys. Polon. **A67**, 385 (1985).
[29]C. Verie, F. Raymond, C. Rigaux, A. Kozacki, and I. Vacquie, in Proceedings of the 15th International Conference on the Physics of Semiconductors, Kyoto, 1980 [J. Phys. Soc. Jpn. A **49**, 771 (1980)].
[30]G. Bastard, Y. Gouldner, C. Rigaux, N'Guyen Hy Han, J. P. Vieren, M. Menant, and A. Mycielski, Phys. Lett. **46A**, 99 (1973).
[31]W. Knap, I. Roschger, W. Szuszkiewicz, H. Kreen, A. M. Witowski, and M. Grynberg, in *Proceedings of the 17th International Conference on the Physics of Semiconductors,* edited by J. D. Chadi and W. A. Harrison (Springer-Verlag, Berlin, 1985), p. 659.
[32]M. Dobrowolska, W. Dobrowolski, M. Otto, T. Dietl, and R. R. Galazka, in Proceedings of the 15th International Conference on the Semiconductors, Kyoto, 1980 [J. Phys. Soc. Jpn. A **49**, 815 (1980)].
[33]C. Finck, S. Otmezguine, G. Weill, and C. Verie, in *Proceedings of the 11th International Conference on the Physics of Semiconductors* (Polish Scientific, Warszawa, 1972), p. 944 and see, e.g., references to Ref. 30.
[34]The resonant acceptor states were observed mainly in HgTe and HgTe-based mixed crystals. Their existence can be found in transport measurements (Ref. 29), in magnetooptical experiments (Ref. 30), and transmission data, where the transition occurs from an ionized level to the conduction band (Ref. 31). Experimental evidence of such states was also reported for $Hg_{1-x}Mn_xTe$ (Ref. 32) and $Hg_{1-x}Cd_xTe$ (Ref. 33).
[35]R. R. Galazka, W. Dobrowolski, and J. Thuillier, Phys. Status. Solidi B **98**, 97 (1980).
[36]A. M. Witowski and M. Grynberg, Phys. Status Solidi B **100**, 389 (1980).
[37]W. Szuszkiewicz and A. M. Witowski, Solid State Commun. **48**, 821 (1983).
[38]Because of $E_F > E_A$ for HgSe it is impossible to observe the acceptor state in interband magnetotransmission experiments or in the behavior of mobility vs free-carrier concentration as in HgTe (Ref. 29). Suggestions concerning the existence of resonant states are from observations of additional oscillations in Shubnikov–de Haas experiments (Ref. 35), but one cannot establish the energy of the impurity level. From the interpretation of FIR reflectivity data (Ref. 36) one can assume the existence of an additional density of states in the conduction band. To explain the free-carrier absorption due to photon-ionized impurity-plasmon processes (Ref. 37), one has to assume a compensation ratio of about 50%. This means an acceptor concentration of the order of 10^{16} cm^{-3}. It should be pointed out once more that the above-mentioned results are not direct evidence for the existence of a resonant acceptor level in HgSe, only a suggestion.
[39]G. Bastard, C. Rigaux, Y. Couder, H. Thome, and A. Mycielski, Phys. Status Solidi B **94**, 205 (1979).